

# Modeling of radiative heat transfer from a solid cylindrical flame and mass transfer in forest fire network

K. Khelloufi<sup>#1</sup>, Y. Baara<sup>#2</sup>, N. Zekri<sup>#3</sup>

<sup>#</sup>*Department of physics, University of Sciences and Technology Oran  
LEPM, BP 1505 El Mnaouer, Oran, Algeria*

<sup>1</sup>*ph\_khadij@hotmail.fr*

<sup>2</sup>*baara.yamina@gmail.com*

<sup>3</sup>*nzekri@yahoo.fr*

**Abstract**— The dynamics on the non-equilibrium propagation in a two-dimensional network modeling wildfire propagation was studied. The model includes deterministic long-range interactions due to radiation and a time weighting procedure and a probabilistic long-rang connection due to the spotting process. The estimation of the emitted flux is based on modelling of the shape of the flame. In our model we use an homogenous cylindrical shape to calculate the surface flux emitted into the space using a Monte Carlo method (MMC). While in the probabilistic connections, we use an exponential distribution of shortcuts or firebrands [1].

Three weight-dependent propagation regimes were found: dynamical, static, and non-propagative [2]. The dynamical regime shows saturation for small weight values and a percolation transition area depending on the weight and size of the interaction domain. A discussion is provided on how the weighting procedure and deterministic long-range interaction can affect the propagation. For the probabilistic connections, a minimum percolation threshold is observed. This minimum threshold is a scaling effect of the system.

The model, applied here to forest fire propagation with a minimum computation time with respect to the real time (100 times), could be used in many other fields..

**Keywords**— Small world network; Fire spread; Wild land fire; Firebrands; Thermal radiation

## I. INTRODUCTION

Phase transitions take an important place in physics; they describe the dynamic or static transition from one phase to another. Although they have been studied for several decades some problems remain open such as the universality and the spread dynamics at the phase transition ([2]-[5]).

The percolation model is now applied to several fields of physics ranging from electronic and optical properties of composite materials to the behavior of epidemics through forest fires ([2]-[6]).

Watts and Strogatz introduced in 1998 a new network model called: Small World Network (SWN) to describe the social networks ([6],[7]). It is based on a regular network

where a probability  $\phi$  of shortcuts or links connecting randomly any cells of the network is included [7].

Recently, the SWN model was adapted to fire propagation ([2], [5], [8]-[10]). In this model, two kinds of long-range interactions were considered: a deterministic one due to the ignition by flame radiations and a probabilistic one due to the spotting process caused by firebrands emission ([11], [12]).

In fact, in forest fire network, the nature of the produced flames is diffusive, which lead to a convective and radiative heat transfer to the unburned area. A portion of the energy released from these thermal degradation is transferred by convection in the smoke plume witch contain some of ignited particles named firebrands.

Another portion is lost by radiation process outside of the flame in the environment or to the fuel. The radiative emission is largely responsible on the spread of large fires (Munoz, Planas, Ferrero, & Casal, 2007), and it mainly depends on the combustion temperature, the composition of the flame and the soot content [2].

The aim of this work is to determine the emitted flux of cylindrical solid flame to use in our simulation next to the spotting process. Furthermore we examine the influence of both deterministic and probabilistic long-range connections on wild land fire spread and percolation.

## II. MODEL DESCRIPTION

A variant of the Watts–Strogatz SWN model is proposed. It is built from a two-dimensional  $L$  sized lattice composed of identical square cells of size  $a$ . A proportion  $p$  of these cells is occupied by the fuel, the remaining cells being empty.

Two kinds of long-range connections are considered: one due to radiation flux within an ignition influence zone, and a second one due to the spotting process caused by firebrand emission throughout the network (see fig. 1).

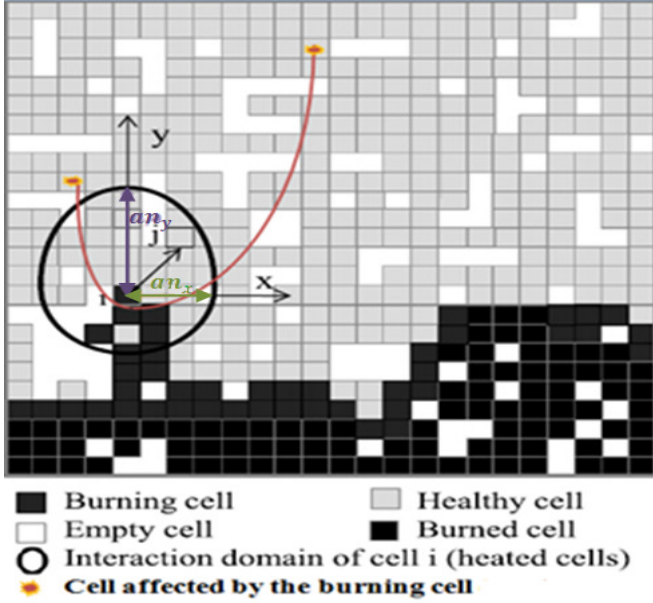


Fig. 1 The small world network model

The influence zone is characterized by two length scales  $l_x$  and  $l_y$ . In the case of isotropic propagation, the influence zone has a circular shape ( $l_x=l_y$ ). The anisotropy of the influence zone (and front shape) is induced by the terrain slope and/or the wind speed (chosen here in the  $y$ -direction). In this case the influence zone becomes elliptic with an eccentricity defined by the anisotropy ratio  $AR = l_y/l_x$ .

The radiation flux  $P_{ij}$  received by a healthy cell  $j$  located in the interaction domain of a burning cell  $i$  is determined using a cylindrical flame shape [10]:

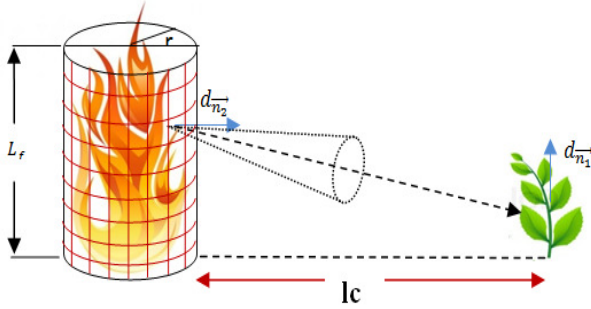


Fig. 2 Modeling the radiation emission of a cylindrical flame

Using a Monte Carlo simulation, we are able to count the total number of emitted quantum in the direction of propagation by each isothermal surface element  $dA_i$ [9]:

$$q = \frac{Q_{dA_i}}{N_i} = \frac{E(T_i)dA_i}{N_i} \quad (01)$$

Where,  $N_i$  is the quantum ( $i$ ) of the elements  $dA_i$ .

These number lead to the exact expression of the emitted flux:

$$dQ_{dA_i} = \frac{qN_i}{\pi} \cos \theta \sin \theta d\theta d\psi \quad (02)$$

Taking into account the boundary condition of the MMC, the random number used in this method are given by [10]:

$$\begin{cases} R_\theta(x) = \int_0^x 2 \sin x \cos x dx = \sin^2 x \\ R_\psi(y) = \frac{Y}{2\pi} \end{cases} \quad (03)$$

Where:  $0 \leq R_\theta(x)$  et  $R_\psi(y) \leq 1$

According to Y. Billau [11], these emitted flux is function of the traveled distance, it decay in square only for flames of a point-like shape. While, for another configuration it decay with different exponents. So the radiation flux is generally power-law decreasing with an exponent  $\beta$  depending on the distance to the fuel as shown in fig. 3 for a cylindrical flame

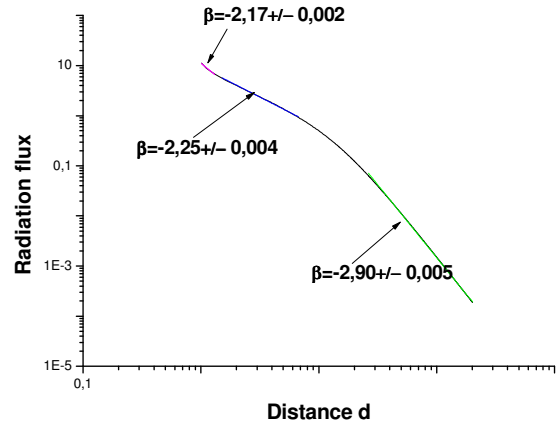


Fig. 3 Radiation flux power-law decreasing with the distance  $D_{ij}$

These power law behavior is expressed by the equation (04) using our network parameter.

$$P_{ij} = \frac{P_0}{\left( \left( \frac{x_{ij}}{l_x} \right)^2 + \left( \frac{y_{ij}}{l_y} \right)^2 \right)^{\frac{\beta}{2}}} \quad (04)$$

$x_{ij}$  and  $y_{ij}$  are the distances to the flame in  $x/y$ - direction and  $P_0$  is the minimum radiation flux received by a cell which can lead to its ignition.

Each cell is ignited when its energy reaches the ignition energy  $E_{ign}$ . As the flame has a finite combustion time  $t_c$ , a weighting process is thus defined by the ratio  $R = \frac{E_{ign}}{P_0 t_c}$  [1].

Three propagation regimes were found [2]; a dynamical regime for  $R < R_c$  ( $R_c$  being the critical weight above which there is no propagation) with a saturation behavior for  $R \leq 1$  where a burning cell ignites completely its influence zone. At  $R = R_c$  (called the static regime), the only the nearest neighbor cell is ignited by the burning cell during its

combustion time  $t_c$ . Above  $R_c$  the system no propagation is possible.

The spotting process [12] occurs under the action of wind when the burning brush and trees have a high plume of flame ( $\approx 3\text{m}$ ) [12].

These incandescent or burning particles (e.g., pieces of bark, pine needles, twigs, leaves and fragments of cork...) may give rise to some secondary fires far from the main fire front [10].

The ability of firebrands to set off new fires depends primarily on their internal energy for the landing. It depends on wind speed, the terrain slope and the nature of the fuel [12]. In addition to these parameters, the number of emitted firebrands influences fire propagation.

Firebrand emission is an important phenomenon which should be taken into account for fighting strategy. This subject has thus received a considerable attention of scientists to determine the characteristics and structure of fire spread [12].

The firebrand's emission probability was found both theoretically [12] and experimentally [1] to decrease exponentially with the distance within an angle of  $\alpha = \frac{\pi}{3}$  in the wind direction.

$$\mathcal{P} = \mathcal{P}_0 \text{Exp}\left(-\frac{d}{D_0}\right) \quad (05)$$

Where  $\mathcal{P}_0$ , is the average emission probability per cell,  $d$  the distance traveled by a single firebrand and  $D_0$  the characteristic emission distance defined by equation 3.

### III. RESULTS

#### A. Validation of MMC:

The modeling and estimation of the emitted flux emitted by a flame is based on the counting of the number of quanta forming these flux. The minimization of fluctuations is necessary to determining the right number of quanta emitted which gives the best flux behavior.

In our case, we took a cylindrical flame of a height  $h = 10\text{m}$  and radius  $r = 1$ , the results of radiative flux emitted by the flame is shown in the following figure (Fig. 4)

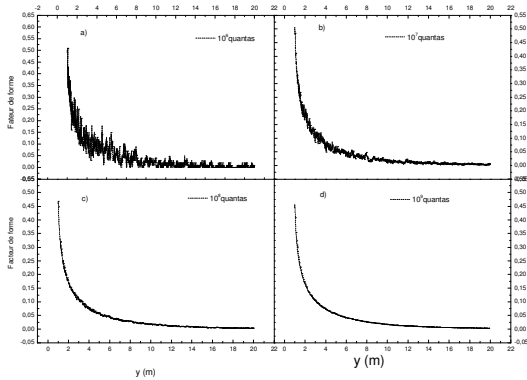


Fig. 4 Radiation emitted flux of a cylindrical flame of a height  $h=10\text{m}$  and a radius  $r=1\text{m}$

In Fig. 4, we note that the increment in the number of quantum emitted decreases fluctuations, then we can say that the most appropriate number for the minimum fluctuations is  $10^8$  quantum's/m<sup>2</sup> it up.

The value of the radiative flux emitted from a straight cylindrical flame depends essentially on the form factor (impact factor) defined between the flame and the responsive element.

The results of the form factor obtained by our Monte Carlo simulation for a cylindrical flame of a height  $h = 14\text{m}$  and radius  $r = 4$  is in agreement with experiment C. Joly, E. Bernuchon [13] (Fig. 5):

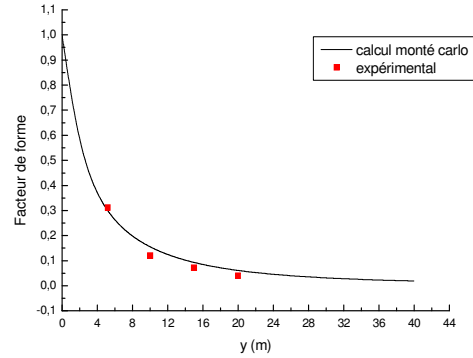


Fig. 5 Impact factor for a straight cylindrical flame obtained by MMC and experience.

#### B. Radiation effect

We use a square network of  $300 \times 300$  cells randomly occupied with a probability  $p$ . The percolation threshold  $p_c$  corresponds statistically to the appearance of a cluster of burned cells connecting the opposite sides of the heterogeneous system. As the propagation /non-propagation transition is a second order phase transition, the threshold corresponds to the maximum disorder. The maximum propagation time fluctuations are used for this end.

The effects of the weighting process and the deterministic long-range connections on the percolation threshold are examined. In the dynamical regime ( $R < R_c$ ), the percolation threshold  $p_c$  is independent of the interaction exponent  $\beta$  within the statistical errors (see fig. 6). In the saturation regime ( $R \leq 1$ ),  $p_c$  is independent of the weight  $R$ . This confirms the universality of this phase transition at  $p_c$ . As  $R$  approaches  $R_c$  and for  $\beta = 3$ ;  $p_c$  reaches unity due to the strength of anisotropy which makes the propagation nearly 1D.

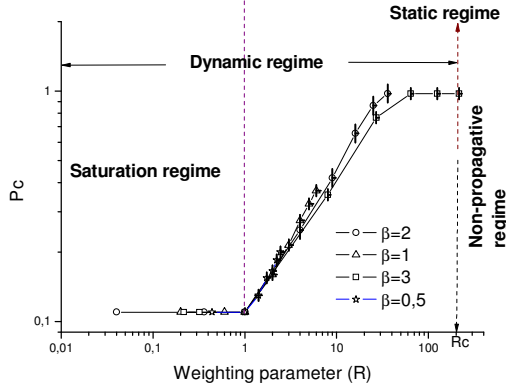


Fig. 6 The percolation threshold  $p_c$  versus  $R$  for  $l_y=6a$ ,  $l_x=2a$  and  $\beta=0.5, 1, 2$  &  $3$ . The error bars are shown.

The static regime corresponds to the case where the influence zone is reduced to the nearest neighbor. It is defined by

$$R_c \propto \left(\frac{l_y}{a}\right)^\beta \quad (06)$$

For  $R > R_c$ , the receptive cell will not reach its ignition energy  $E_{ign}$  before the emitting cell stops burning ( $t_c$ ). There is thus no propagation in this regime.

### C. Spotting process

Let us now consider the spotting process. The traveled distance of a firebrand depends on the characteristic distance  $D_0$ . The percolation threshold dependence on  $D_0$  is shown in Fig. 7.

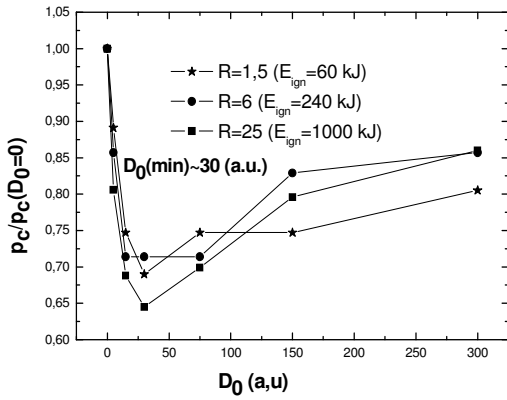


Fig. 7  $p_c^{SWN}/p_c^{RN}$  versus  $D_0$  for  $l_y = 6a$ ,  $l_x = 2a$  and  $R=1.5, 6$  &  $25$ ,  $L=300a$ .

From Fig. 7, there is a minimum percolation threshold (here for  $D_0=30a$ ). This minimum depends only on the system size. It disappears for an infinite system.

The scaling behavior of the propagation time fluctuations at  $p_c$  has nearly a linear shape (see Fig. 8):

$$\delta t_{max} = v_{p_c} L + b \quad (07)$$

Where  $v_{p_c}$  is the rate of spread at  $p_c$ .

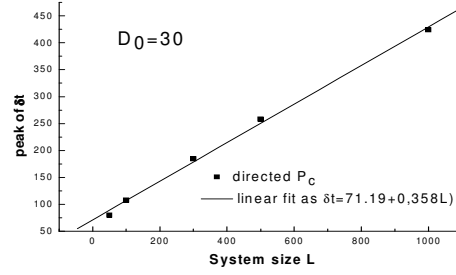


Fig. 8  $\delta t$  versus the size  $L$  (the line is a fit the data).

This behavior of the correlation time induces a new set of dynamical exponents which characterizes the spread in the non-equilibrium systems. Such study will be considered in the future.

The number of emitted firebrands in the network depends on the flame intensity [10]. This number corresponds here to  $\mathcal{P}_0$ . If  $\mathcal{P}_0 < 1$ , this number becomes the emission probability per cells.

The number of effective firebrands depends on the size of the network with [9]:

$$\begin{cases} D_0 \gg L & N_{fb}(t) = cN_{bs}(t) \frac{L}{D_0} \\ D_0 \ll L & N_{fb}(t) = cN_{bs}(t) \end{cases} \quad (08)$$

$N_{bs}$  is the number of burning cells.

The effective firebrand induces secondary fires which contribute in the global process of spreading. As the average emission probability  $\mathcal{P}_0$  increases, the contribution of the secondary fire increase and the percolation threshold decrease (see Fig. 9).

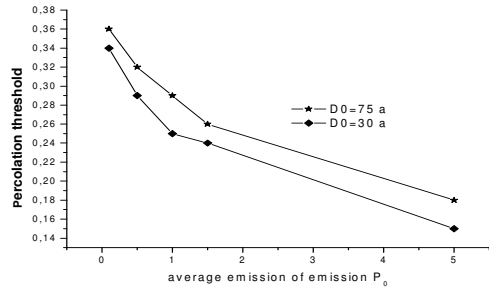


Fig. 9  $p_c$  versus  $\mathcal{P}_0$  for  $D_0=0, 30$  and  $75m$

## IV. CONCLUSION

- We have used a forest fire model to study the effect of heat transfer -flame radiation- and mass -spotting process- on the percolation transition.
- We found that the flux radiation is a power law function of the traveled distance.
- The dependence of the distance to the radius and height of the flame was mounted in this work; we also studied the effect of this dependence on the phase transition percolating / no-percolating.

- We have shown that the dynamics of the spread of fire is independent of the flux emitted by the flames (radiative interaction), it just depends on the effect of weighting  $R$ .
- We found the  $p_c$  behavior independent on the power radiation exponent  $\beta$ , within the errors.
- Due to size effects, the probabilistic long-range connection (spotting process) leads to a minimum percolation threshold.
- The contribution of the secondary fire induced by the spotting process activates the spread and decreases the percolation threshold value.

## REFERENCES

- [1] [www.ffp.csiro.au/nfm/fbm/vesta/spotfire.html](http://www.ffp.csiro.au/nfm/fbm/vesta/spotfire.html)
- [2] N.Zekri, K.Khelloufi, L.Zekri, B.Porterie, A.Kaiss and J.P.Clerc, Phys. Lett. A **376**, 2522-2526, 2012.
- [3] D.Stauffer and A.Aharony, "Introduction to Percolation Theory", 1<sup>st</sup>ed Taylor and Francis, London, 1992.
- [4] G.Grimmett, "Percolation" Springer-Verlag, Heidelberg, 1999
- [5] N.Zekri, B.Porterie, J.P.Clerc, and J.C. Loraud, Phys. Rev. E **71**, 046121, 2005.
- [6] D.J.Watts, "Small Worlds: The Dynamics of Networks between Order and Randomness" Princeton University Press, Princeton, NJ, 1999.
- [7] D.J.Watts, S.H.Strogatz, Nature **393**, 440-442, 1998.
- [8] B.Porterie, A.Kaiss, J.P.Clerc, L.Zekri, and N.Zekri, Appl .Phys. Lett. **93**, 204101, 2008.
- [9] J.K.Adou, Y.Billaud, D.A.Brou, J.P.Clerc, J.L.Consalvi, A.Fuentes, A.Kaiss, F.Nmira, B.Porterie, L.Zekri, N.Zekri, Ecological Modelling **221**, 1463-1471, 2010.
- [10] B.Porterie, N.Zekri, J.P.Clerc, J.C.Loraud, Combustion and Flame **149**, 63-78, 2007.
- [11] Y.Billaud, A.Kaiss, J.L.Consalvi and B.Porterie, Int.J.Therm.Science **50**, 2, 2011.
- [12] J.L.Consalvi, P.Mindykowski, J.P.Vantelon, B.Porterie, Fire Safety Journal **46**, 48-55, 2011 and References therein.
- [13] C. Joly, E. Bernuchon, *Méthode pour l'évaluation et la prévention des risques accidentels*, U-2 Feux de nappe, INERIS report DRA-006, 2002